

Published in final edited form as:

Cancer Res. 2008 October 1; 68(19): 7932–7937. doi:10.1158/0008-5472.CAN-08-0866.

Validation of the p21-activated kinases as targets for inhibition in neurofibromatosis type 2

Chunling Yi¹, Erik W. Wilker², Michael B. Yaffe², Anat Stemmer-Rachamimov³, and Joseph L. Kissil^{1,4}

¹Molecular and Cellular Oncogenesis Program, The Wistar Institute, Philadelphia, Pennsylvania 19104, USA

²Center for Cancer Research, Massachusetts Institute of Technology, Cambridge, Massachusetts

³Department of Pathology, Massachusetts General Hospital, Boston, Massachusetts

Abstract

Neurofibromatosis type 2 (NF2) is a dominantly inherited cancer disorder caused by mutations at the *NF2* gene locus. Merlin, the protein product of the *NF2* gene, has been shown to negatively regulate Rac1 signaling by inhibiting its downstream effector kinases, the p21-activated kinases (Paks). Given the implication of Paks in tumorigenesis, it is plausible that merlin's tumor suppressive function might be mediated, at least in part, via inhibition of the Paks. We present data indicating this is indeed the case. First, analysis of primary schwannoma samples derived from NF2 patients showed that in a significant fraction of the tumors, the activity of Pak1 was highly elevated. Second, we employed shRNAs to knockdown Pak1, 2 and 3 in NIH3T3 cells expressing a dominant-negative form of merlin, NF2^{BBA} (NIH3T3/NF2^{BBA}) and find that simultaneous knockdown of Pak1–3 in these cells significantly reduced their growth rates in vitro and inhibited their ability to form tumors in vivo. Finally, while attempting to silence Pak1 in a rat schwannoma cells, we found that these cells were unable to tolerate long-term Pak1 inhibition and rapidly moved to restore Pak1 levels by shutting down Pak1 shRNA expression through a methylation-dependent mechanism. These data suggest that inhibiting Pak could be a beneficial approach for the development of therapeutics towards NF2. In addition, the finding that the shRNA-mediated Pak1 suppression was silenced rapidly by methylation raises questions about the future application of such technologies for the treatment of diseases such as cancer.

Keywords

Neurofibromatosis type 2 (NF2); merlin; p21-activated kinase (Pak); Rac1; shRNA

Introduction

The hallmark of neurofibromatosis type 2 (NF2), which affects 1 in 30,000–40,000 of the population, is the development of bilateral vestibular schwannomas (VS) at the eighth cranial nerve. Most NF2 patients go on to develop multiple cranial and spinal schwannomas, meningiomas and, less frequently, intra-spinal ependymomas, with symptoms including auditory, visual and motor impairments. Currently, risky surgical excision is the only treatment option. And the tumors will inevitably recur, leading to a high early mortality rate among NF2 patients (1).

⁴Corresponding author. Wistar Institute, 3601 Spruce St. Philadelphia, PA., 19104. Email E-mail: jkissil@wistar.org.

Merlin, the protein encoded by the NF2 gene, is closely related to the ERM proteins (ezrin, radixin and moesin), containing an N-terminal FERM domain followed by a coiled-coil domain. The carboxyl-terminal domain (CTD) of merlin is unique and lacks the conventional actin-binding motif found in ERM proteins. Merlin CTD can associate with its N-terminal FERM domain, forming a “closed” and functionally active configuration. Phosphorylation of merlin at serine 518 disrupts this intra-molecular interaction and suppresses its growth inhibitory activity. This phosphorylation is mediated by p21-activated kinases (Paks), which bind to activated (GTP-bound) Rac/Cdc42 and function as their direct effectors (2,3). In addition, it has been shown that merlin S518 can also be phosphorylated by the cAMP-dependent protein kinase (PKA), whereas its dephosphorylation involves the myosin phosphatase (MYPT-1-PP1delta) (4,5).

Several lines of evidence indicate that merlin is not only regulated by the Rac-Pak axis but also functions as an inhibitor of Rac signaling. Specifically, merlin overexpression suppresses Rac1-induced activation of c-Jun-N-terminal kinase (JNK) and AP-1 transcriptional activity, while loss of merlin results in the opposite (6). In addition, merlin inhibition via dominant-negative mutants or siRNA enables Rac1 recruitment to plasma membrane and alleviates contact inhibition in confluent cells (7). Furthermore, increased levels of activated Rac with disrupted temporal control have been reported in primary NF2-mutant schwannoma cells (8, 9). Finally, merlin overexpression in Schwann cells suppresses Pak1 activity, whereas ablation of merlin in MEFs leads to Pak1 activation (7,10,11). The inhibitory activity of merlin towards Pak1 has been attributed to its direct interaction with the Rac-binding domain of Pak1, which interferes with the binding of activated Rac to Pak1 (10,12).

In this study, we examine whether inhibiting Pak can reverse the transformed and cancer phenotypes that arise from NF2 deficiency. We find that Pak1 is hyperactive in primary schwannomas isolated from NF2 patients and that suppression of the Paks via shRNAs reduces the ability of NF2 mutant cells to grow in vitro and form tumors in a xenograft model of NF2.

Materials and Methods

Schwannoma biopsies

Frozen tissue samples from NF2 patients that underwent surgery in Massachusetts General Hospital (MGH), were received from the MGH Brain Tumor tissue repository, under the approval of the MGH Institutional Review Board.

2-dimensional gel analysis

Frozen tumor samples were minced and protein was extracted in sample buffer (9.8 M Urea, 2% CHAPS, 5ml 0.5% IPG buffer 4–7, DTT 15 mg/ml). All subsequent steps were performed as previously described (10).

Cell culture conditions

RT4 and NIH3T3 cells were grown in low-glucose DME, 10% fetal calf serum, 1x non-essential amino acids and 100 IU/ml penicillin-streptomycin. Transfections were performed with Lipofectamine2000 (Invitrogen), following manufacturer’s instructions. To inhibit DNA methylation, 5-aza-2’-deoxycytidine (Sigma) was added to the media (5 ng/ml).

Knockdown of Pak1, 2, 3 using lentiviral delivered shRNAs

For silencing endogenous Pak1, 2 and 3 in NIH3T3 and RT4 cells, several sequences were tested and the following targeting sequences were selected based on their knockdown efficiency: Pak1: “5’-GGATTCTGTGCACAGATAA” and “5’-GGAATGGATGGCTCTGTCA”; Pak2: “5’-GAGATTATGGAGAAATTAA”; Pak3: “5’-

GGAATTAATTATTAATGAA". DNA oligos containing individual targeting sequences were cloned into pLenti-lox3.7 (pLL3.7) as previously described (13). The resulting vectors were co-transfected with packaging vectors VSVG and Δ8.9 into 293T cells and viral supernatant was collected 48 and 72 hrs post transfection. For infection, cells were incubated with the viral supernatant overnight and infected cells (GFP-positive) were selected by flow cytometry.

Western blot analysis

Protein extracts were prepared with RIPA lysis buffer (50 mM TRIS-HCl, pH 7.5, 1% Nonidet P-40, 0.25% sodium deoxycholate, 150 mM NaCl, 1 mM EGTA, 1 mM sodium orthovanadate, and 1 mM NaF). The following antibodies were used according to manufactures' instructions: Pak1 (N-20), Pak3 (N-19), merlin (C-18)- Santa Cruz; Pak2 (2608) - Cell signaling; α-tubulin (AC42) and β-actin (AC40) - Sigma.

Cell proliferation assays

30,000 cells/well were plated in 12-well dishes in triplicate for each cell line. At indicated time points, cells from individual wells were trypsinized and counted using a Coulter counter (Z1 series, Beckman Coulter). Cells were fed every 3 days throughout the assay. Statistical analysis was performed using Student's t-test.

Tumorigenicity assays

Cells were trypsinized, washed, and resuspended at 10^7 cells/ml in PBS. 10^6 cells (100 μl) were injected subcutaneously into the flanks of 5 week-old nude mice (BALB/c nu/nu, Jackson Laboratories). Mice were monitored and tumor diameters were measured weekly following injections.

Bisulphite Sequencing

Genomic DNA was first digested with Sac I, precipitated and dissolved in ddH₂O. 1 μl of 6N NaOH was added to 19 μl ddH₂O containing 2 μg of the digested DNA, and incubated at 37 °C for 15'. Subsequently, 120 μl bisulphite conversion solution (107 μl 4.04M NaHSO₃, 7 μl 10 mM Hydroquinone, and 6 μl 6N NaOH) was added to the DNA solution and bisulphite conversion was carried out (30" at 95 °C followed by 15' at 50 °C for 15 cycles). Bisulphite treated DNA was then desalted (Wizard DNA cleanup kit - Promega) and eluted in 50 μl TE buffer. 2.5 μl of 6N NaOH was added to the eluted DNA and incubated at RT for 5'. DNA was precipitated and resuspended in 30 μl ddH₂O. 1 μl was used as template in a 20 μl nested PCR reaction with the following primers: "5'-TTTAAAAGAAAAGGGGGGATT" and "5'-TCTCAAACACACAATTACT". 1 μl of the first round was used as template for a second round of PCR using the nested primers: "5'-AGGGGAAAGAATAGTAGATATAA" and "5'-TTAACCRAAACAAAAATAACC". The resulting PCR product was purified and sequenced using primer "5'-AGGGGAAAGAATAGTAGATATAA".

Senescence-Associated β-Gal Assay

Cells were washed three times with PBS and fixed with 0.2% glutaraldehyde for 5'. After three washes with PBS, cells were incubated overnight with X-gal solution (1 mg/ml X-gal, 150 mM NaCl, 2 mM MgCl₂, 5 mM K₃Fe(CN)₆, 5 mM K₄Fe(CN)₆, and 40 mM NaPi, pH 6.0) at 37 °C.

Results

Elevated levels of Pak1 activity in primary schwannoma tumor samples

The activation of Pak1 involves its phosphorylation at multiple sites (10,14,15). We have previously established a 2-dimensional (2-D) gel approach to monitor the phosphorylation state

of Pak1, which has been shown to accurately reflect the activation state of Pak1 in the cell (7,10). By use of this approach, we examined the status of Pak1 in primary schwannoma samples isolated from NF2 patients. Myelinated nerve from a patient with wild-type NF2 was used as control. As shown in Fig 1A, Pak1 migrates as a single spot towards the neutral pH range in “normal” myelinated nerve, indicating that Pak1 is mostly unphosphorylated/inactive. In contrast, with the exception of sample xt3224, 18 of the 19 schwannoma samples we analyzed displayed various forms of phosphorylated Pak1 (Fig 1A and 1B), indicative of Pak1 activation. In 6 of the 19 samples, as exemplified by sample xt1441, the majority of the Pak1 proteins existed in highly acidic forms, suggestive of hyper-phosphorylation (Fig 1A and 1B). In 12 of the 19 samples, multiple forms of hypo- or hyper-phosphorylated Pak1 were present, as represented by sample xt1729. These data suggest that in primary tumors from NF2 patients, Pak1 exists in a phosphorylated/activated form. This is consistent with previous findings that merlin acts as a direct inhibitor of Pak1 (7,10).

shRNA-mediated depletion of Pak1, 2, and 3 inhibits the proliferation and tumorigenicity of NIH3T3/NF2^{BBA} cells

We have previously demonstrated that expression of NF2^{BBA}, a dominant-negative form of merlin, in NIH3T3 cells induced transformation, loss of contact inhibition and tumor formation when injected in nude mice (16). Since Pak1 is the most abundant member of the Pak family in NIH3T3 cells, we first examined the effect of Pak1 inhibition in these cells. We infected wild-type NIH3T3 or NIH3T3/NF2^{BBA} cells with either an empty lentiviral vector or vectors harboring Pak1 specific small hairpin RNAs (shRNA) and selected infected (GFP-positive) cells by flow cytometry. As shown in Fig 2A, Pak1 protein levels were significantly reduced in cells infected with lentiviruses carrying Pak1 shRNAs. Following the growth kinetics of these four different cell lines, we found that, consistent with previous findings, NIH3T3/NF2^{BBA} cells grow faster than wild-type NIH3T3 cells (Fig 2B). However, we observed no significant differences in growth rates between cells infected with empty vectors and those with Pak1 shRNAs (Fig 2B). We injected these four cell lines into nude mice and found that NIH3T3/NF2^{BBA} cells expressing Pak1shRNAs still developed tumors of similar size compared with control NIH3T3/NF2^{BBA} cells (Fig 2C). Therefore, inhibition of Pak1 alone is not sufficient to counter the effect of merlin impairment in NIH3T3/NF2^{BBA} cells. Similar results were obtained when either Pak2 or Pak3 was knocked down individually in NIH3T3/NF2^{BBA} cells (Supplementary figure 1).

Since Pak1, 2 and 3 share high sequence homologies, we reasoned that the loss of individual Pak is likely compensated by the other two members of Paks. To investigate this possibility, we infected NIH3T3 with lentiviruses carrying shRNAs specific for Pak1, Pak2 and Pak3. As shown in Fig 3A, these NIH3T3 cells showed significant reduction of all three Paks. We characterized the respective proliferation kinetics of NIH3T3 and NIH3T3/NF2^{BBA} cells infected with control lentiviruses or those expressing shRNAs against Pak1–3. In contrast to the lack of effect observed in Pak1 ablation alone, knockdown of all three Paks dramatically reduced the growth rates of the NIH3T3/NF2^{BBA} cells (Fig 3B and supplementary Fig 1), indicating that depletion of all three Paks successfully reversed the hyperproliferative effect of mutant merlin in our cellular model. Knockdown of Pak1–3 also decreased the proliferation rate of wild-type NIH3T3 cells, but to a much lesser extent, comparing to the dramatic effects observed in the NIH3T3/NF2^{BBA} cells (Fig 3B).

We next injected NIH3T3/NF2^{BBA} cells carrying empty vectors or Pak1–3 shRNAs side by side into the flanks of nude mice and followed the development of tumors over the course of several weeks. In agreement with our previous study (16), the control NIH3T3/NF2^{BBA} cells (left flank) quickly developed into tumors, reaching an average diameter of 160 mm by 3 weeks post injection (Fig 3C, supplementary Table 1). In comparison, NIH3T3/NF2^{BBA} cells

expressing Pak1–3 shRNAs (right flank) resulted in either no tumors or much smaller tumors at a considerably delayed rate. The average diameter of tumors that eventually developed from these cells was close to 10 mm at 3 weeks post-injection (Fig 3C, supplementary Table 1). These results indicate that simultaneous suppression of all three Paks can at least partially inhibit the ability of Nf2^{BBA} to induce tumor formation in a xenograft model of NF2, which corroborate our hypothesis that inhibiting Paks could serve as a potential treatment for NF2.

To investigate what caused the eventual development of small tumors from injected NIH3T3/NF2^{BBA} cells expressing Pak1–3 shRNAs in some of the mice, we isolated the tumors from both flanks of these mice and examined the expression levels of Pak1, 2, and 3. As shown in Fig 3D, in two of the mice examined (#7007 and #7049), the expression of at least two of the Paks was partially restored to similar levels of those in tumors from control NIH3T3/NF2^{BBA} cells. This may explain why these cells did eventually form tumors. In a third mouse (#7045), the levels of all three Paks remained low in the tumor developed from Pak-shRNA expressing NIH3T3/NF2^{BBA} cells (Fig 3D), indicating that additional mechanisms involved in offsetting the loss of Pak in these cells.

Schwannoma cells are dependent on Pak1 and silence Pak1 shRNA expression via de novo methylation

Because NF2 patients primarily develop Schwann cell tumors, we next examined the effect of Pak knockdown in a well-characterized rat schwannoma cell line, RT4. Unlike NIH3T3 cells in which all three Paks are expressed, RT4 cells express predominantly Pak1 (supplementary Fig 2). We infected RT4 cells with lentiviruses carrying the same Pak1-specific shRNAs that were used in NIH3T3 cells (Fig 2 and Fig 3), and as expected, RT4 cells showed significantly reduced Pak1 expression following the infection (Fig 4A). However, the Pak1 levels in RT4 cells infected with Pak1 shRNAs were quickly restored, within 2–3 passages, to similar levels found in control RT4 cells (Fig 4A). Correspondingly, the expression level of GFP, a positive selection marker in the lentiviral vector, pLenti-lox3.7, into which Pak1 shRNAs were cloned, dropped rapidly during the first 2–3 passages of the infected RT4 cells (Fig 4A).

Given the rapid nature of restoration in Pak1 levels and concurrent down-regulation of GFP expression, we suspected that RT4 cells might have employed an epigenetic mechanism, namely DNA methylation, to silence Pak1 shRNA expression and restore levels of Pak1. To test whether this is indeed the case, we carried out bisulphite sequencing to directly examine the methylation status on the approximately 200 bp promoter region in pLenti-lox3.7 that drives Pak1 shRNA expression. As shown in Fig 4B, multiple CpG sites were indeed methylated within this relatively small region in high passage RT4 cells carrying pLenti-Pak1 shRNAs. To further confirm that methylation is responsible for silencing Pak1 shRNA expression, we added the methylation inhibitor 5-aza-2'-deoxycytidine (5-aza) into the cell culture medium of RT4 cells carrying empty vectors or Pak1 shRNAs, which had been passed at least 8 times and displayed similar Pak1 expression levels (Fig 4C). The cells were cultured for several days in the presence of 5-aza and Pak1 expression levels were examined at different time points. In contrast to what we observed with these cells without 5-aza treatment (Figure 4A), after only a single day of 5-aza treatment, Pak1 levels were significantly lowered in RT4 cells carrying Pak1 shRNAs when compared to control RT4 cells (Fig 4C). We were able to sustain this suppression of Pak1 expression for at least 3 days of treatment (Fig 4C). Thus, RT4 cells evade Pak1 inhibition by shutting down Pak1 shRNA expression through methylation of the pLenti-lox3.7 promoter.

We then measured the growth rates of RT4 cells carrying empty vectors or Pak1 shRNAs in the presence or absence of 5-aza. In the absence of 5-aza, RT4 cells infected with Pak1 shRNAs showed only slightly reduced growth rate compared to control RT4 cells (Fig 4D). In the presence of 5-aza, control RT4 cells grew relatively slower than untreated cells (Fig 4D). This

is not surprising, considering that 5-aza is a global methylation inhibitor. In sharp contrast, however, RT4 cells carrying Pak1 shRNAs completely failed to grow under culture conditions that included 5-aza (Fig 4D). The difference is also obvious in the morphologies of these cells. Compared to the mostly spindle-shaped untreated or 5-aza treated control RT4 cells, the Pak1-shRNA infected RT4 cells grown in the presence of 5-aza are enlarged and flattened, displaying a morphology consistent with cellular senescence (Fig 4E). These cells also stained positive for the senescence-associated expression of β -galactosidase activity, indicating that sustained expression of Pak1 shRNAs in RT4 cells leads to inhibition of Pak1 expression, resulting in cellular senescence (Fig 4E). Importantly, RT4 cells transiently transfected with Pak1 siRNAs, which should not be susceptible to methylation-mediated silencing, did not proliferate during the first few days post transfection (supplementary Fig 2A). Consistent with the notion that Pak1 is the dominant Pak in RT4 cells, co-transfection of Pak2 siRNAs with Pak1 siRNAs failed to further reduce the growth rate of RT4 cells (supplementary Fig 2B). Taken together, we concluded that RT4 cells require Pak1 for proliferation and quickly move to silence Pak1 shRNA expression through de novo methylation.

Discussion

We have shown for the first time that Pak1 is highly activated in primary schwannomas from NF2 patients. This is consistent with our hypothesis that merlin functions as a tumor suppressor by blocking Pak activation. Employing both cellular and animal models, we directly tested this hypothesis. We found that the simultaneous knockdown of all three Paks is required to counter the hyperproliferation and tumor-forming capacity of NIH3T3 cells harboring the NF2^{BBA} allele. Taken together, these results validate Paks as potential targets for the development of NF2 therapeutics.

Previous studies have linked Pak1 to cancer and transformation and utilization of Pak inhibitors to reverse cellular transformation have also been reported (17) (18,19). However, these studies are inconclusive, as the inhibitors employed are broad-range kinase inhibitors that do not specifically inhibit Paks. Therefore, the important next step is to develop specific Pak inhibitors and test them in cellular and animal models of NF2. Another interesting finding in this study is that different cell types respond differently to Pak1 inhibition. While knockdown of Pak1 is inconsequential in NIH3T3 cells (Fig 2), Pak1 ablation in RT4 cells leads to growth arrest (Fig 4D, supplementary Fig 2). In addition, NIH3T3 cells maintained reduced Pak1 expression mediated by Pak1 shRNAs even after over 20 passages (data not shown), whereas RT4 cells quickly silenced Pak1 shRNA via de novo methylation (Fig 4A and 4B). These differences suggest that while Pak1 is probably the dominant Pak in RT4 cells, it functions redundantly with Pak2 and Pak3 in NIH3T3 cells. However, since Pak1, 2 and 3 are highly homologous, especially within their catalytic domains, it is most likely that any Pak inhibitors will work equally well on all three Pak isoforms. Therefore, these cell type differences in Pak function should not affect the effectiveness of Pak inhibitors.

Finally, virus-delivered small hairpin RNAs have been proposed as a potential therapeutic tool in treating human diseases such as cancer (20). As described in this study, an shRNA targeting an essential gene, in our case, Pak1 in RT4 cells, can be silenced directly by DNA methylation. Further research should be carried out to investigate whether other cell types can also employ similar mechanisms to silence stably integrated foreign shRNA and how frequently such events can occur. Addressing these questions would be prudent before any future application of such technologies as a treatment modality.

Supplementary Material

Refer to Web version on PubMed Central for supplementary material.

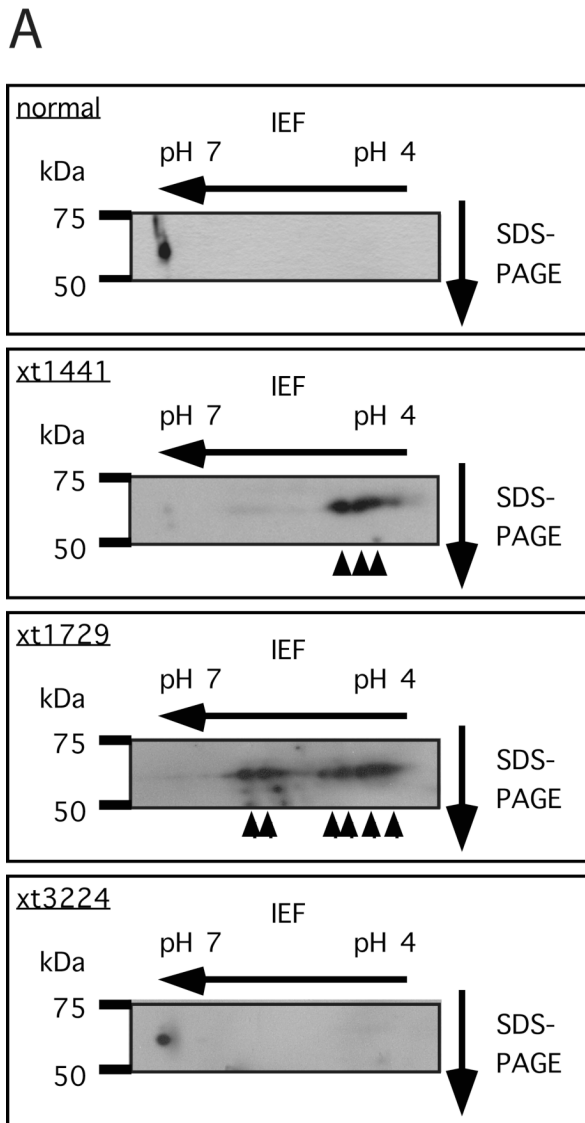
Acknowledgments

This work is supported in part by the Department of Defense Neurofibromatosis Research Program. C.Y. is a recipient of Ruth L. Kirschstein NRSA fellowship. We thank Dr. Joanne Thorvaldsen for advice on bisulphite sequencing.

References

1. Yohay KH. The genetic and molecular pathogenesis of NF1 and NF2. *Semin Pediatr Neurol* 2006;13:21–26. [PubMed: 16818172]
2. Kissil JL, Johnson KC, Eckman MS, Jacks T. Merlin phosphorylation by p21-activated kinase 2 and effects of phosphorylation on merlin localization. *J Biol Chem* 2002;277:10394–10399. [PubMed: 11782491]
3. Xiao GH, Beeser A, Chernoff J, Testa JR. p21-activated kinase links Rac/Cdc42 signaling to merlin. *J Biol Chem* 2002;277:883–886. [PubMed: 11719502]
4. Alfthan K, Heiska L, Gronholm M, Renkema GH, Carpen O. Cyclic AMP-dependent protein kinase phosphorylates merlin at serine 518 independently of p21-activated kinase and promotes merlin-ezrin heterodimerization. *J Biol Chem* 2004;279:18559–18566. [PubMed: 14981079]
5. Jin H, Sperka T, Herrlich P, Morrison H. Tumorigenic transformation by CPI-17 through inhibition of a merlin phosphatase. *Nature* 2006;442:576–579. [PubMed: 16885985]
6. Shaw RJ, Paez JG, Curto M, et al. The Nf2 tumor suppressor, merlin, functions in Rac-dependent signaling. *Dev Cell* 2001;1:63–72. [PubMed: 11703924]
7. Xiao GH, Gallagher R, Shetler J, et al. The NF2 tumor suppressor gene product, merlin, inhibits cell proliferation and cell cycle progression by repressing cyclin D1 expression. *Mol Cell Biol* 2005;25:2384–2394. [PubMed: 15743831]
8. Kaempchen K, Mielke K, Utermark T, Langmesser S, Hanemann CO. Upregulation of the Rac1/JNK signaling pathway in primary human schwannoma cells. *Hum Mol Genet* 2003;12:1211–1221. [PubMed: 12761036]
9. Nakai Y, Zheng Y, MacCollin M, Ratner N. Temporal control of Rac in Schwann cell-axon interaction is disrupted in NF2-mutant schwannoma cells. *J Neurosci* 2006;26:3390–3395. [PubMed: 16571745]
10. Kissil JL, Wilker EW, Johnson KC, Eckman MS, Yaffe MB, Jacks T. Merlin, the product of the Nf2 tumor suppressor gene, is an inhibitor of the p21-activated kinase, Pak1. *Mol Cell* 2003;12:841–849. [PubMed: 14580336]
11. Morrison H, Sperka T, Manent J, Giovannini M, Ponta H, Herrlich P. Merlin/neurofibromatosis type 2 suppresses growth by inhibiting the activation of Ras and Rac. *Cancer Res* 2007;67:520–527. [PubMed: 17234759]
12. Hirokawa Y, Tikoo A, Huynh J, et al. A clue to the therapy of neurofibromatosis type 2: NF2/merlin is a PAK1 inhibitor. *Cancer J* 2004;10:20–26. [PubMed: 15000491]
13. Rubinson DA, Dillon CP, Kwiatkowski AV, et al. A lentivirus-based system to functionally silence genes in primary mammalian cells, stem cells and transgenic mice by RNA interference. *Nat Genet* 2003;33:401–406. [PubMed: 12590264]
14. Buchwald G, Hostinova E, Rudolph MG, et al. Conformational switch and role of phosphorylation in PAK activation. *Mol Cell Biol* 2001;21:5179–5189. [PubMed: 11438672]
15. Chong C, Tan L, Lim L, Manser E. The mechanism of PAK activation: autophosphorylation events in both regulatory and kinase domains control activity. *J Biol Chem* 2001;276:22222–22228. [PubMed: 11438672]
16. Johnson KC, Kissil JL, Fry JL, Jacks T. Cellular transformation by a FERM domain mutant of the Nf2 tumor suppressor gene. *Oncogene* 2002;21:5990–5997. [PubMed: 12203111]
17. Tang Y, Chen Z, Ambrose D, et al. Kinase-deficient Pak1 mutants inhibit Ras transformation of Rat-1 fibroblasts. *Mol Cell Biol* 1997;17:4454–4464. [PubMed: 9234703]
18. Vadlamudi RK, Adam L, Wang RA, et al. Regulatable expression of p21-activated kinase-1 promotes anchorage-independent growth and abnormal organization of mitotic spindles in human epithelial breast cancer cells. *J Biol Chem* 2000;275:36238–36244. [PubMed: 10945974]
19. Howe AK, Juliano RL. Regulation of anchorage-dependent signal transduction by protein kinase A and p21-activated kinase. *Nat Cell Biol* 2000;2:593–600. [PubMed: 10980699]

20. Lu PYXF, Woodle MC. In vivo application of RNA interference: from functional genomics to therapeutics. *Adv Genet* 2005;54:117–142. [PubMed: 16096010]



Sample ID	Pak1 phosphorylation
normal	-
xt660	+
xt1377	+
xt1386	+
xt1441	++
xt1567	+
xt1635	+
xt1681	++
xt1729	++
xt3005	++
xt3044	+
xt3148	+
xt3224	-
xt3421	+
xt3571	+
xt3639	+
xt3668	+
xt3681	++
xt3799	++
xt3853	+

“-”: unphosphorylated only;
 “+”: hypo- and hyper- phosphorylated;
 “++”: hyper-phosphorylated only.

Figure 1. Pak1 is activated in schwannomas from NF2 patients

A, analysis of Pak1 activation by 2-D gel electrophoresis coupled to western blot analysis. Arrowheads indicate the various phosphorylated forms of Pak1. **B**, summary of Pak1 phosphorylation status in primary schwannomas. All samples were normalized for variations in sample loading by comparison to actin as an internal standard.

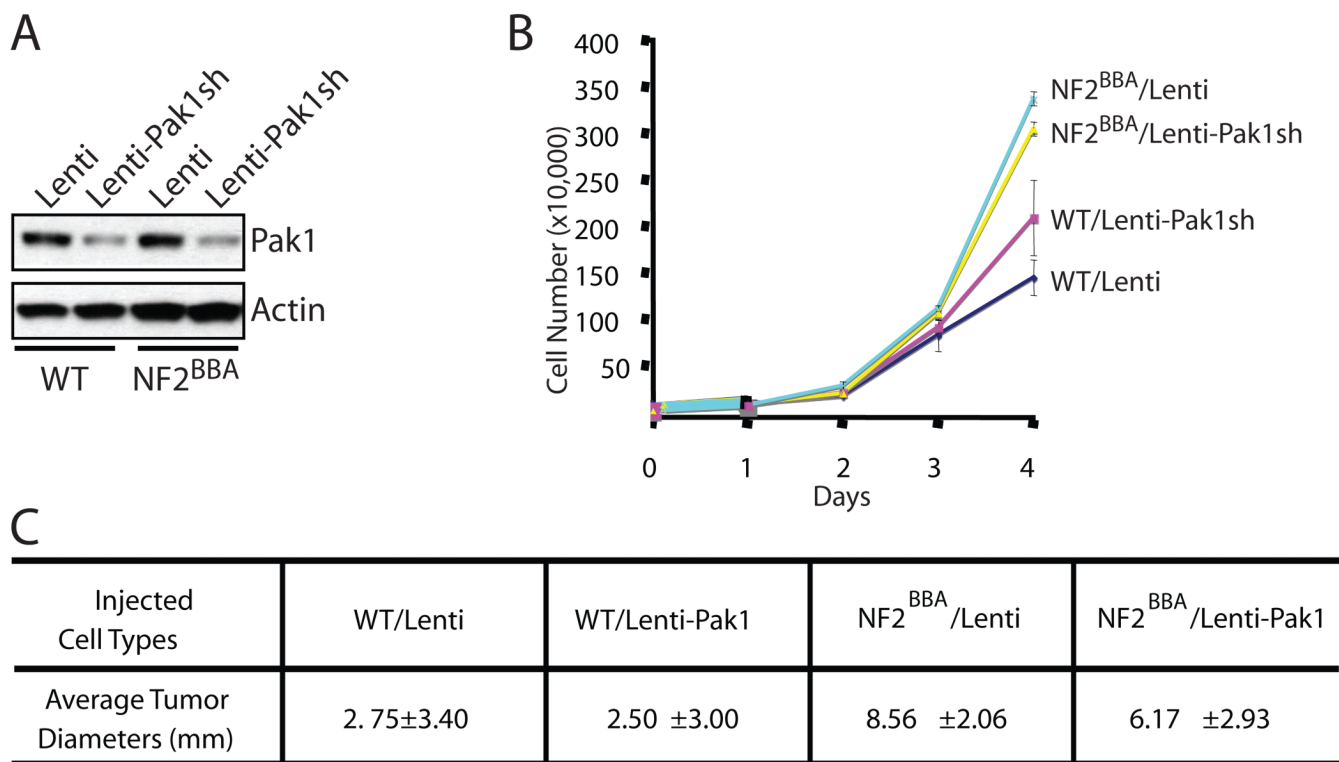


Figure 2. Pak1 knockdown on NIH3T3 cells is insufficient to inhibit cell transformation due to impaired NF2 function

NIH3T3 (WT) or NIH3T3/NF2^{BBA} (NF2^{BBA}) cells were infected with empty lentiviruses (Lenti) or lentiviruses harboring Pak1 shRNAs (Lenti-Pak1sh). **A**, Pak1 expression levels were determined by western blot analysis. Actin was used as an internal standard. **B**, cellular proliferation kinetics. 3×10^4 cells from each of the cell types above were plated in triplicate into 12-well plates. Cells were harvested and counted at day 0, 1, 2, 3 and 4. The data are representative of 3 independent experiments. Error bars show standard deviation (SD). **C**, tumor formation capability. 10^6 cells were injected into the rear flanks of SCID mice. Four mice were used for each cell line. Tumors were measured 15 days after injections.

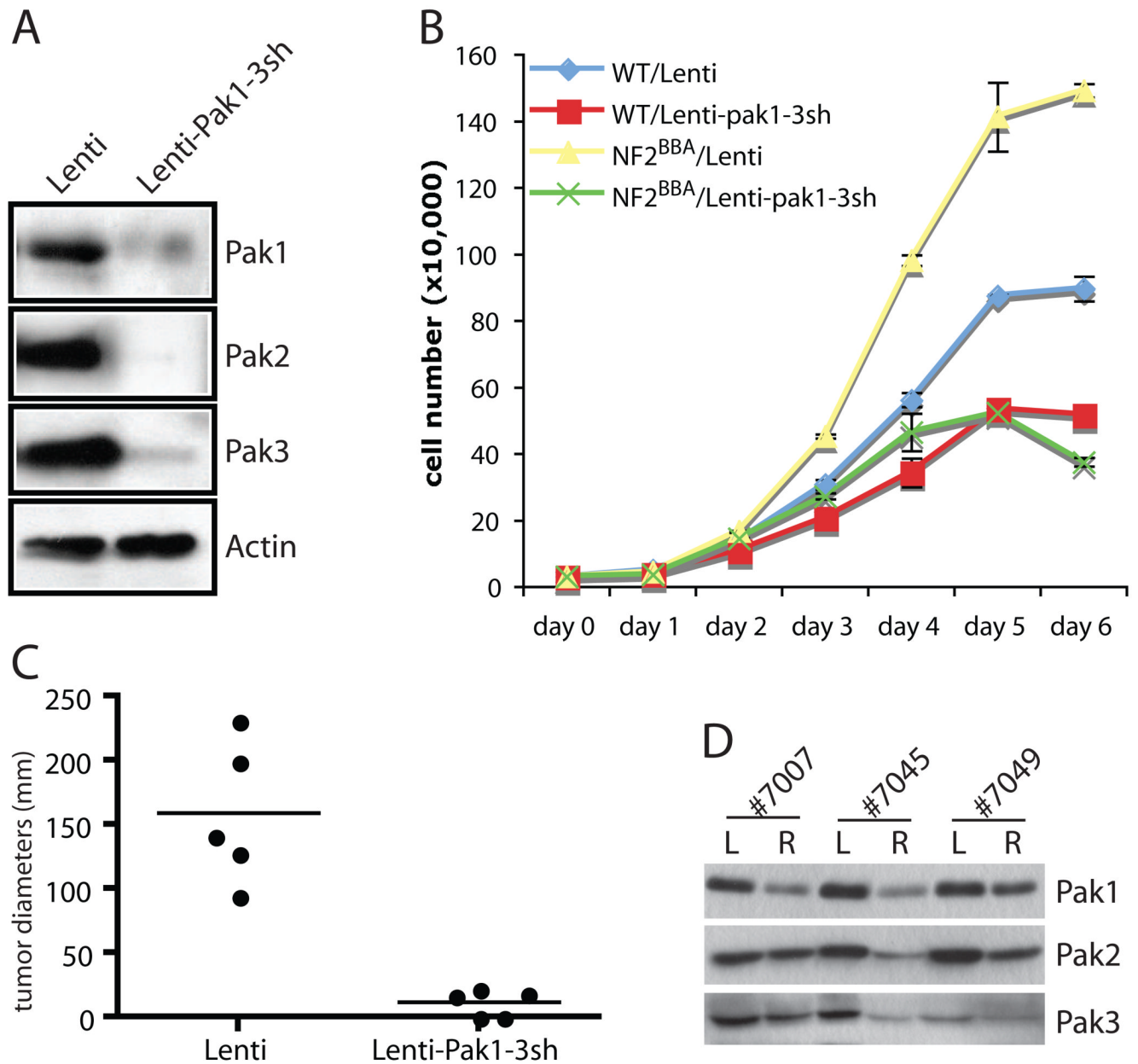


Figure 3. Knockdown of Pak1–3 is sufficient to inhibit cellular transformation due to impaired NF2 function

The effects of simultaneous Pak1+2+3 knockdown were examined in NIH3T3 (WT) or NIH3T3/NF2^{BBA} (NF2^{BBA}) cells infected with empty lentivirus (Lenti) or lentiviruses harboring Pak1+2+3 shRNAs (Lenti-pak1-3sh). **A**, western blot analysis of Pak1, 2 and 3 levels. Actin was used as an internal standard. **B**, assessment of cellular proliferation. 3×10^4 cells were plated in triplicate into 12-well plates. Cells were harvested and counted at day 0, 1, 2, 3, 4, 5, and 6. The data is representative of 3 independent experiments. Error bars show standard deviation (SD). **C**, tumor size distribution in SCID mice. Tumor formation was assessed by injecting 5×10^5 NIH3T3/NF2^{BBA} cells infected with empty virus (Lenti) to the left flanks and 5×10^5 of NIH3T3/NF2^{BBA} -Lenti-PAK1-3sh into the right flanks of the same mice. Five mice were used in total. The size of tumors was measured 23 days after injection.

Horizontal lines represent average tumor diameters. **D**, western blot analysis of tumors dissected from mice #7007, #7045, and #7049. L: tumors from left flank arising from NIH3T3/NF2^{BBA}-Lenti cells R: tumors from right flank arising from NIH3T3/NF2^{BBA}-Lenti-PAK1-3sh cells.

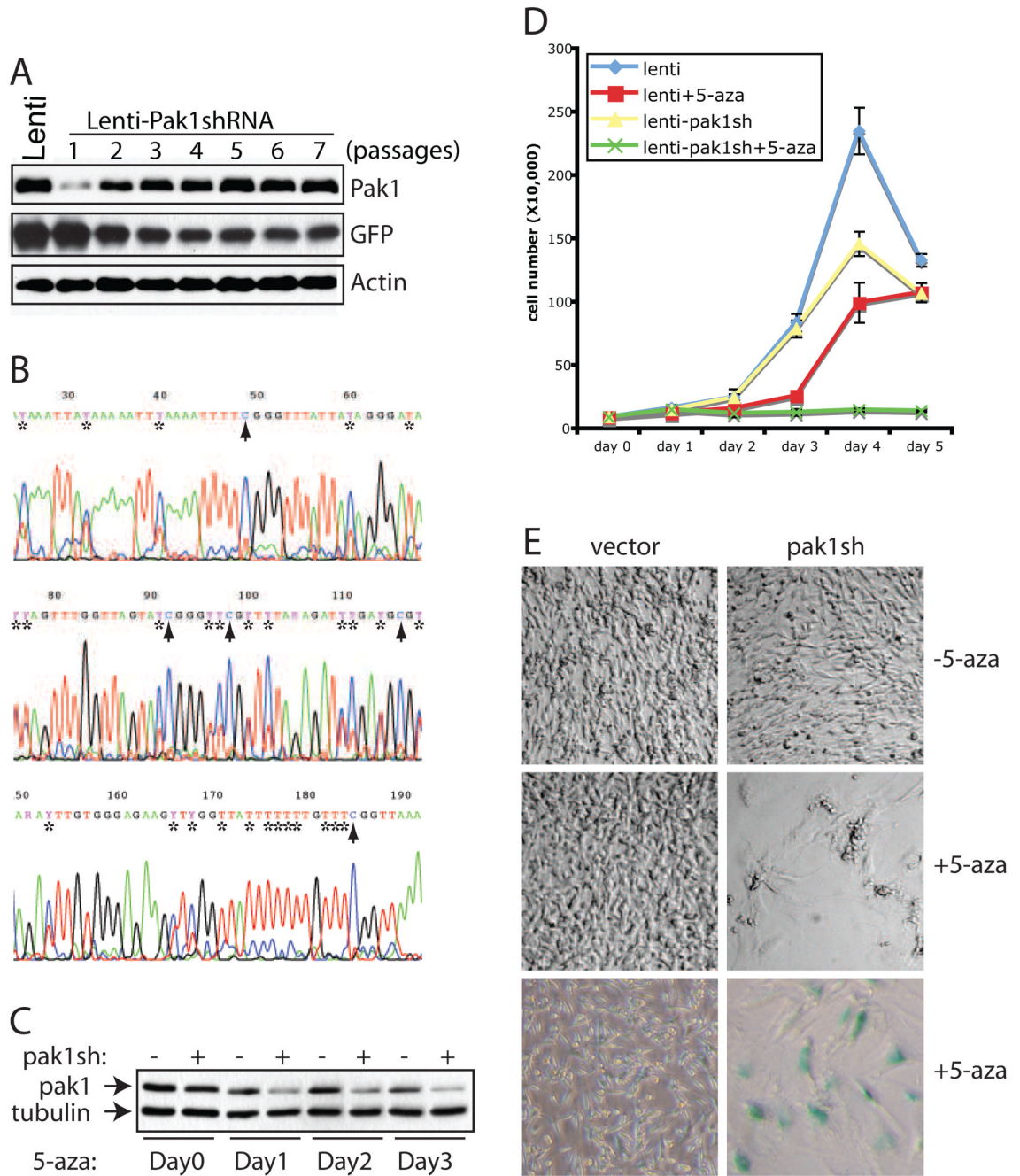


Figure 4. Rat schwannoma cells are dependent on Pak1 expression

A, western blot analysis of Pak1 expression in RT4 cells at various passages after infection with lentiviruses harboring a Pak1 specific shRNA. RT4 cells infected with empty lentivirus vector (Lenti) were used as control. Actin serves as an internal loading control. **B**, methylation analysis of Lenti-shPak1 promoter in RT4 cells. The genomic DNA was isolated from RT4 cells at passage 6 following infection with lentiviruses harboring a Pak1 specific shRNA and subjected to bisulphite conversion, methylation specific PCRs and direct sequencing. “*”s mark the cytosines in the original sequence that have been completely or partially converted to uracils, whereas arrowheads indicate unconverted/methylated cytosines. **C**, western blot analysis of Pak1 expression in RT4 cells infected with empty lenti vector (–) or Pak1shRNA

(+) treated with 5-aza. The 5-aza was added to the culture medium at 5 ng/ml final concentration. The cells were harvested and analyzed at day 0, 1, 2, and 3 into the treatment. **D**, assessment of cellular proliferation. 4×10^4 cells were plated in triplicate into 12-well plates and cells were harvested and counted at day 0, 1, 2, 3 and 4. The data is representative of 3 independent experiments. Error bars show standard deviation (SD). **E**, images of RT4 cells infected with vector or Pak1shRNA after 3 days of culture in the presence (+5-aza) or absence (-5-aza) of 5-aza. In the bottom panel, RT4 cells were first fixed and stained with X-gal. Images were taken using Nikon Coolpix 995 digital camera under Leica DM1L light microscope at 10x magnification.